105 (2026) 107173

Contents lists available at ScienceDirect

Poultry Science

journal homepage: www.elsevier.com/locate/psj

Full-Length Article

Single-cell transcriptomic profiling of the chicken spleen reveals cell-type-specific immune responses to *Salmonella* infection

Ping Wang [1], Ruizhi Chen [1], Kai Ren, Xinyu Pu, Jilong Ren, Wuqiang Huo, Fei Wang [*]

Key Laboratory of Animal Genetics, Breeding and Reproduction of Shaanxi Province, College of Animal Science and Technology, Northwest A&F University, Yangling 712100, China

ARTICLE INFO

Keywords:
Chicken
Single-cell RNA sequencing
Salmonella
Immune cell
Gene expression

ABSTRACT

Although the spleen is a key immune organ, the dynamic remodeling of its cellular landscape during development and the heterogeneous immune responses of these cells to avian *Salmonella* infection remain to be elucidated. In this study, we reanalyzed publicly available datasets comprising 116,791 single-cell transcriptomes from the chicken spleen. We annotated a total of 40 distinct cell types, systematically delineating the cellular composition and dynamic changes from embryonic to adult stages. Moreover, single-cell comparisons before and after *Salmonella* infection revealed markedly strengthened intercellular crosstalk within the lymphoid lineage and between lymphoid and myeloid lineages. Transcriptional analysis demonstrated that naive T cells, NK2 cells, and B cells underwent the most extensive transcriptional remodeling, implying their pivotal roles in the antibacterial immune response. Of note, the responses of different immune cell subsets displayed both subset-specific patterns and shared features. Furthermore, notable differences were detected in cellular interaction networks, as well as in the gene expression profiles of NK2 cells and activated T cells between different chicken breeds, which may serve as potential molecular mechanisms underlying the divergent disease resistance phenotypes among chicken breeds. Collectively, these findings provide a comprehensive temporal atlas of chicken splenic development and immunity, offering valuable insights into the molecular basis of disease resistance and laying a theoretical foundation for poultry breeding strategies.

Introduction

The spleen serves as the central blood-borne immune organ in poultry and plays an indispensable role in maintaining immune homeostasis and defending against pathogen invasion (Doan et al., 2022). During embryogenesis, its acts as a primary hematopoietic organ supporting the generation and differentiation of hematopoietic progenitors, thus laying the foundation for early immune cell development (Guo et al., 2025; Xie et al., 2024). In adulthood, it functions primarily as a secondary lymphoid organ dedicated to immune surveillance, blood filtration and the orchestration of adaptive immune responses (Golub et al., 2018). However, the dynamics of cellular composition from the embryonic stage to adulthood remain largely unknown. Characterizing the developmental trajectory of splenic cellular architecture is essential for understanding avian immune ontogeny.

Salmonella represents one of the most prevalent bacterial pathogens in poultry production. Following ingestion, *Salmonella* invades the host via the digestive tract and disseminates to colonize and replicate in multiple tissues and organs (Sharma et al., 2025). Such invasion triggers intestinal inflammation and systemic infection, resulting in compromised growth performance and even mortality. Beyond its detrimental impacts on poultry production, *Salmonella* infection also constitutes a severe threat to food safety through the consumption of contaminated meat and eggs (Barrow and Neto, 2011; Wigley, 2014). Consequently, a comprehensive understanding of the host immune response to *Salmonella* infection is of critical importance. Previous studies have demonstrated that *Salmonella* infection elicits marked alterations in the transcriptional profile of the spleen (Matulova et al., 2012). However, most existing investigations rely on bulk RNA sequencing (Matulova et al., 2012; Elsharkawy et al., 2022), which obscures the inherent cellular heterogeneity of the spleen and fails to distinguish the specific responses of individual immune cell subsets following *Salmonella* infection. Consequently, bulk RNA sequencing is limited in their ability to resolve cell-type-specific immune dynamics, leaving the precise

* Corresponding author.
E-mail address: wangfei2840@nwafu.edu.cn (F. Wang).
[1] These authors contributed equally to this work.

https://doi.org/10.1016/j.psj.2026.107173
Received 2 April 2026; Accepted 24 May 2026
Available online 25 May 2026

contributions of distinct splenic lineages to host defense largely uncharacterized (Tzec-Interián et al., 2025). In contrast, single-cell technologies enable high-resolution characterization of cellular heterogeneity within tissues and permit direct comparison of cell-type-specific gene expression programs before and after infection, thereby revealing shared and divergent immune responses across cell populations (Papalexi and Satija, 2018; Nadukkandy et al., 2025; Pan et al., 2025). A recent single-cell study has explored splenic cellular heterogeneity and differentiation trajectories of distinct cell subtypes, as well as alterations in cell proportions between Cobb broilers and Beijing-You chicks before and after infection (Zhang et al., 2025). However, the gene expression patterns and intercellular communication dynamics across different cell types in response to *Salmonella* infection remain largely uncharacterized.

To address these knowledge gaps, the present study aims to construct a comprehensive single-cell transcriptomic atlas of the chicken spleen across embryonic and adult developmental stages. Specifically, we uncover infection-induced alterations in gene expression programs and intercellular communication networks across distinct immune cell subsets and identify breed-associated differences in transcriptional and cellular interaction profiles that may underpin divergent disease responses. By integrating these multi-dimensional analyses, we establish a foundational framework for understanding the cellular and molecular basis of *Salmonella* infection in chickens, thereby providing actionable insights for poultry breeding and disease control strategies.

Materials and methods

scRNA-Seq data processing

We downloaded single-cell RNA sequencing data of Hy-Line Brown laying hens at multiple developmental stages (embryonic days 13, 16 and 21, and 14 weeks post-hatch) from previous research (Wang et al., 2026)(PRJNA1125639, https://www.ncbi.nlm.nih.gov/bioproject/?term=PRJNA1125639). Additionally, we downloaded single-cell datasets for Beijing-You chicks and Cobb broilers at 31 days of age, comprising both healthy controls and *Salmonella*-infected groups from another research (Zhang et al., 2025)(PRJNA1013511, https://www.ncbi.nlm.nih.gov/bioproject/?term=PRJNA1013511). After the filtering of raw sequencing reads, reads were aligned to the chicken genome (GCF_016699485.2). Following this processing, gene expression matrices containing gene names, cell barcodes, and raw UMI counts were generated using either the DNBelab C Series single-cell RNA analysis pipeline (https://github.com/MGI-tech-bioinformatics/DNBelab_C_Series_scRNA-analysis-software) or Cell Ranger software. These datasets were subsequently imported into R to construct Seurat objects with the Seurat package (version 4.4.0) (Butler et al., 2018). Quality control was performed independently for each sample, in which cells were retained for further analysis only if they expressed more than 500 genes, fewer than the 95th percentile of total genes, and exhibited mitochondrial gene content below 15%.

Following quality filtering, the raw count matrix was normalized using the *"LogNormalize"* method with a scale factor of 10,000, and the top 2,000 highly variable genes were identified using the *"FindVariableFeatures"* function with the *"vst"* (variance stabilizing transformation) selection method. After principal component analysis (PCA), batch effects across samples were corrected using the Harmony algorithm implemented in Seurat, with default parameter settings (theta = 2, lambda = 1) (Korsunsky et al., 2019). The resulting Harmony embeddings were used to construct a shared nearest neighbor (SNN) graph via the Seurat functions "FindNeighbors" (dims = 1:15) and "FindClusters" (resolution = 0.5). UMAP visualization was generated based on the first 15 Harmony dimensions with a minimum distance parameter of 0.10.

Cluster-specific marker genes were identified using "*FindAllMarkers*", with thresholds of adjust p-value < 0.05 and $|\log_2 FC| > 0.25$. Finally, each cluster was annotated based on the expression of established marker genes. The expression patterns of marker genes were visualized using the DotPlot or DoHeatmap function. Based on the single-cell annotation results for each group, the cell count of each cell type was quantified and its proportion was calculated. To construct the splenic single-cell atlas, we utilized samples from Hy-Line Brown laying hens and healthy individuals of both Beijing-You chicks and Cobb broilers. Subsequently, we used the Cobb broilers datasets to characterize alterations in gene expression profiles and intercellular communication networks following *Salmonella* infection. Furthermore, we compared the transcriptional landscapes and cell-cell communication patterns between healthy Beijing-You chicks and Cobb broilers spleens to elucidate breed-specific variations.

Pseudo-time trajectory analysis

To reconstruct the cellular differentiation trajectory, we utilized the Monocle 2 R package (Qiu et al., 2017). This method projects cellular states onto a 2D manifold and orders cells along a pseudotime axis. Key drivers of cell state transitions were identified by detecting genes with significant expression changes along pseudotime via the differentialGeneTest function with default parameters. These genes were further clustered into co-expression modules, and their expression patterns were visualized using the plot_pseudotime_heatmap function to deduce the underlying regulatory programs. Gene expression dynamics during cell state transitions were visualized using the plot_genes_in_pseudotime function.

Identification of differentially expressed genes and pathway enrichment analysis

Differentially expressed genes between the same cell types across different groups were identified using the FindMarkers function in Seurat, with the following parameters: min.pct = 0.1, logfc.threshold = 0.25, and adjusted p-value < 0.05. Gene expression levels of DEGs across different groups were visualized using the VlnPlot function. Intersections among differentially expressed gene sets from distinct cell types were illustrated using UpSetR (v.1.4.0) or VennDiagram (v.1.73).

Gene Ontology pathways analyses were performed was performed using the Metascape network tool (https://metascape.org) (Zhou et al., 2019). Data were further visualized using ggplot2 in R.

Cell–cell interaction analysis

Cellular communication networks among distinct cell types were inferred and visualized using the R package CellChat (Jin et al., 2021). Overexpressed ligands and receptors were first determined using the "identifyOverExpressedGenes" and "identifyOverExpressedInteractions" functions. The communication probability was then calculated via the "computeCommunProb" function to construct intercellular signaling networks. Only ligand-receptor pairs expressed in a minimum of 10 cells were retained using the "filterCommunication" function. Signaling pathway-level communication was further evaluated using the computeCommunProbPathway and aggregateNet functions.

Result

Immune cell types in the chicken spleen at embryonic and adult stages

To investigate the cellular composition of the spleen across developmental stages, we integrated publicly available single-cell RNA sequencing (scRNA-seq) datasets (Zhang et al., 2025; Wang et al., 2026). These datasets included spleen samples collected at embryonic days 13, 16, and 21 (E13, E16, E21; Hy-Line Brown), post-hatch day 31 (D31; Cobb broilers and Beijing-You chicks), and 14 weeks of age (14W; Hy-Line Brown). Notably, although the D31 timepoint included samples collected before and after *Salmonella* infection, only uninfected samples

from all stages were used for integrated analysis. Following rigorous quality control (QC), a total of 92,691 high-quality single cells were retained for downstream analyses, with 15,155, 7,217, 22,294, 31,274, and 16,751 cells derived from E13, E16, E21, D31, and 14W samples, respectively. The mean nFeature and nCount for these cells were 5381 and 1572 (Fig. S1A).

Based on unsupervised clustering and marker gene annotation, we identified 40 distinct cell types (Fig. 1A and Supplementary Fig. 1B), the majority of which were immune populations. These included T cells, B cells, monocytes, macrophages, dendritic cells (DCs), natural killer (NK) cells, as well as their respective subpopulations that represent distinct functional states or proliferative phases. Single-cell profiling of Beijing-You chicks and Cobb broilers were predominantly composed of innate immune cells and mature adaptive immune cells (Fig. 1B-C, and Supplementary Fig. 1C). Besides, single-cell profiling of Hy-Line Brown spleens across developmental stages revealed a progressive increase in the proportions of activated CD8+ T cells, Tregs, and naïve CD8+ T cells from the embryonic to the adult stage (14 weeks), whereas hematopoietic progenitor cells, macrophages, and classical monocytes exhibited a marked decline. These dynamic shifts indicate a functional transition of the spleen from a primary hematopoietic organ in the embryo to a pivotal hub for immune responses in adulthood (Fig. 1D), indicating that the cellular composition of the embryonic spleen differs markedly from that of post-hatch stages. Collectively, these results delineate the core cellular components of innate and adaptive immunity in the chicken spleen across key developmental stages.

Given that the aforementioned splenic cell atlas contains multiple dendritic cells (DCs) subsets, we speculated on the differentiation relationships among these subtypes. Pseudotime analysis predicted a differentiation trajectory from multipotent progenitors (MPP) and DC progenitors to DC1 (Fig. 1E). Along this pseudotime trajectory, we identified a total of 1,708 genes with significant expression changes.

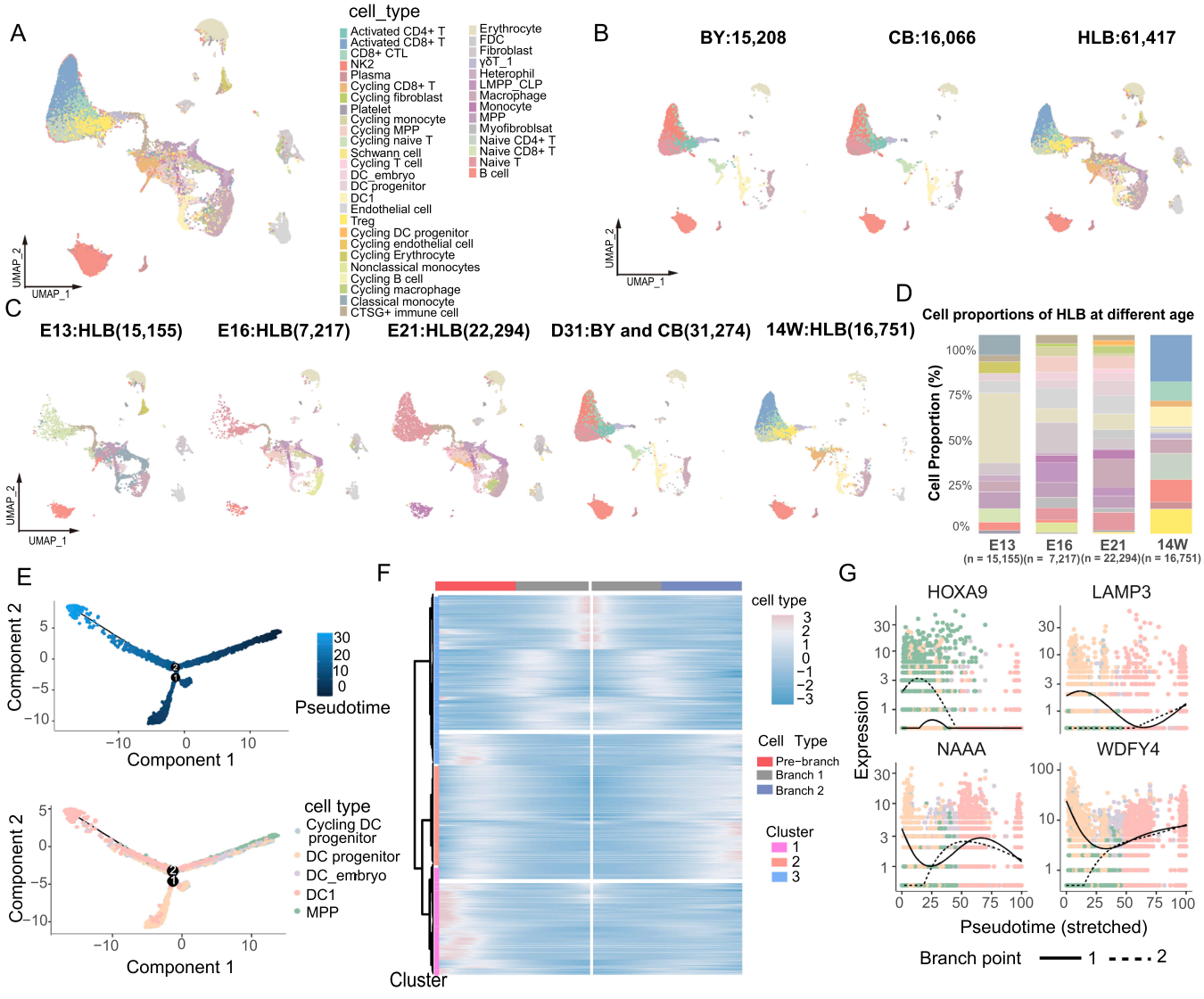

Fig. 1. Single-cell transcriptomic atlas of the chicken spleen across breeds and developmental stages. (A) UMAP projections of all splenic cells colored by annotated cell types. Major populations include T cells, B cells, dendritic cells (DCs), macrophages, progenitor cells, fibroblasts, erythrocytes, and other cell types. (B) UMAP plots showing cell distribution and cluster proportions in the spleen of Beijing-You chicks (BY), Cobb broilers (CB), and Hy-Line Brown (HLB)chickens. (C) UMAP plots showing cell distribution in the spleen at multiple developmental stages (E13, E16, E21, D31, 14 w) across BY, CB, and HLB chickens. (D) Stacked bar plot illustrating the proportion of each cell cluster in the spleen across different ages of HLB chickens (E13, E16, E21, 14W). (E) Pseudotime trajectory analysis of the dendritic cell lineage. Upper panel: cells colored by pseudotime value; lower panel: cells colored by cell type (DC_embryo, DC progenitor, cycling DC progenitor, MPP). (F) Heatmap of cluster-specific gene expression dynamics along pseudotime. (G) Expression trends of selected genes (*HOXA9, LAMP3, NAAA, WDFY4*) along DC pseudotime differentiation. Cells are colored by cell type or branch.

Following clustering analysis, these genes were categorized into three distinct expression modules, each exhibiting stage-specific expression patterns across different pseudotime phases (Fig. 1F). For instance, the expression of *HOXA9* gradually decreased during DC differentiation (Fig. 1G). As a key transcription factor regulating the expansion and differentiation of hematopoietic stem and progenitor cells (Zeng et al., 2021), *HOXA9* was highly expressed in progenitor cells, suggesting its potential role in maintaining early hematopoietic progenitors. In contrast, the expression levels of *LAMP3, NAAA*, and *WDFY4* gradually increased during DC maturation (Fig. 1G). These three genes contribute to the acquisition of antigen-processing and presentation capabilities in DCs, thereby promoting effective T cell activation and adaptive immune responses (Li et al., 2022; Wang et al., 2024; Jo et al., 2025). Their high expression in mature DCs indicates their coordinated roles in regulating DCs functional activation and adaptive immunity.

Alterations in splenic intercellular interactions induced by Salmonella infection

To investigate the effects of *Salmonella* infection on splenic immune cell composition, we analyzed single-cell data from Cobb broilers before and after infection. Specifically, the dataset contained 16,066 cells from uninfected Cobb broilers (CBC: Cobb broilers control) and 17,394 cells from *Salmonella*-infected Cobb broilers (CBS: Cobb broilers with *Salmonella* infection). A total of 14 cell types were identified: naive T, activated CD4+ T, CD8+ CTL, cycling naive T, γδT_1, NK2, B cell, cycling B cell, plasma, DC1, FDC, macrophage, platelet, and erythrocyte (Fig. 2A and Supplementary Fig. 2A). Most cells were lymphoid, while myeloid cells were relatively rare. Analysis of cell-type proportions pre- and post-*Salmonella* infection revealed that within T and NK cell subsets, the frequencies of naive T cells, activated CD4+ T cells, and CD8+ cytotoxic T lymphocytes (CTLs)-were elevated, whereas those of cycling naive T cells and NK2 cells were reduced. In the B cell compartment, the proportion of B cells declined (Supplementary Fig. 2B).

To characterize the impact of *Salmonella* infection on splenic intercellular communication, we analyzed both the number of interactions and interaction strength/weight between immune cell subsets in control (CBC) and infected (CBS) Cobb broilers. In the CBC group, naive T cells, B cells, and NK2 cells exhibited the largest node sizes and most extensive connectivity (Fig. 2B), serving as central hubs in the steady-state immune network. Strong interactions were primarily observed between naive T cells and platelets, as well as between NK2 cells and DC1 (Fig. 2D). Following *Salmonella* infection (CBS), the overall interaction network was markedly remodeled: the total number of intercellular connections increased globally, while the interaction strength of NK2 cells was substantially diminished (Fig. 2C). Notably, interactions of B cells with naive T cells and activated CD4+ T cells significantly enhanced (Fig. 2C). Meanwhile new crosstalk between macrophages and lymphoid subsets (including activated CD4+ T cells and CD8+ CTLs) was amplified (Fig. 2C and D). Furthermore, we observed alterations in ligand-receptor pair interactions following *Salmonella* infection (Fig. 2F and G). For instance, signaling mediated by TNFSF13B-TNFRSF13C was strengthened, suggesting enhanced crosstalk between follicular dendritic cells (FDCs) and B cells upon infection (Fig. 2G). In addition, signaling via TNFSF15-TNFRSF25 was also upregulated (Fig. 2G). Binding of TNFSF15 to TNFRSF25 on lymphocytes delivers co-stimulatory signals to activated lymphocytes (Valatas et al., 2019). Collectively, these results demonstrate that *Salmonella* infection rewires the splenic intercellular communication network, redirecting central immune crosstalk toward lymphoid and myeloid lineages, as well as among lymphoid cell subsets to potentiate adaptive immune activation.

Dynamic transcriptional profiles of T and NK cell subsets upon Salmonella infection

Previous bulk transcriptomic studies have demonstrated that *Salmonella* infection reshapes the host's global gene expression landscape (Oshota et al., 2017). However, the cell-type-specific regulatory features of gene expression during infection remain poorly understood. Here, we systematically characterized the dynamic immune response patterns of distinct cell types to *Salmonella* infection at the single-cell level. Among T cell subsets, naive T cells and activated CD4+ T cells exhibited the most abundant differentially expressed genes (DEGs) pre- and post-infection, with 1,546 and 1,376 DEGs identified, respectively (Fig. 3A-3B and Supplementary Table 1). By comparison, γδT_1, CD8+ cytotoxic T lymphocytes (CTLs), and cycling naive T cells harbored 487, 507, and 735 DEGs, respectively (Supplementary Fig. 3A-C, Supplementary Table 1). For naive T cells, genes highly expressed prior to infection were primarily involved in ubiquitin-dependent protein catabolic processes, regulation of autophagy, and T cell receptor signaling pathways (Fig. 3D). In contrast, genes upregulated after infection were predominantly enriched in cytoplasmic translation, oxidative phosphorylation, and lymphocyte activation (Fig. 3D). For activated CD4+ T cells, genes with high pre-infection expression were mainly associated with T cell activation and cell population proliferation, while those upregulated post-infection were primarily involved in cytoplasmic translation and apoptotic signaling pathways (Fig. 3D).

For NK2 cells, A total of 740 DEGs were identified between control (CBC) and infected (CBS) samples (Fig. 3C and Supplementary Table 1). Genes upregulated following infection were primarily enriched in cytoplasmic translation, inflammatory responses, and activation of the innate immune response, including *HSPA2, HSP90AA1*, and *FSTL4*. In contrast, genes upregulated before infection were significantly enriched in enzyme-linked receptor protein signaling pathways and cell surface receptor protein tyrosine kinase signaling pathways, exemplified by *BACH2, FOXP1, TCF7*, and *IGLL1* (Fig. 3E).

We further systematically analyzed the intrinsic associations among immune response gene sets across distinct cell types. Naive T, activated CD4+ T, and NK2 cells specifically upregulated 120, 256, and 103 genes post-infection, respectively (Fig. 3F). A total of 70 genes were commonly upregulated in both T and NK cell subsets following infection. For instance, *IRF4, JUND, PIK3R1, TNFAIP3, NFKBIA, DAPK1*, and *BIRC2* were among the shared upregulated genes across these cell types (Fig. 3F and G). Among these shared genes, *IRF4* is known to participate in TCR signaling and regulate T cell differentiation (Nayar et al., 2012), while *PIK3R1* is involved in signaling pathways that promote T cell activation (Gutiérrez-Vázquez et al., 2017). Collectively, these results indicate that the immune responses of different cell types to *Salmonella* infection exhibit both shared and cell-type-specific features.

Dynamic transcriptional profiles of B cells and mononuclear phagocytes upon Salmonella infection

Similarly, we investigated transcriptional changes in B cells before and after *Salmonella* infection. Due to the extremely low number of Cycling B cells, differential expression analysis was not performed for this subset. In B cells, we identified a total of 1,076 DEGs, comprising 519 and 557 genes specifically upregulated before and after infection, respectively (Fig. 4A and Supplementary Table 2). These observations indicate that B cells undergo pronounced transcriptional remodeling in response to infection. For example, *BACH2, FOXO1*, and *PAG1* implicated in B cell differentiation and immune homeostasis (Rolland et al., 2011; Igarashi et al., 2014; Szydłowski et al., 2014), exhibited higher expression in pre-infection B cells than in their post-infection counterparts. By contrast, multiple ribosome-related genes-including *RPL17, RPS23, RPS27A, RPS12, RPL19*, and *RPS15*-were upregulated following infection (Fig. 4A), indicative of enhanced protein synthesis. Functional enrichment analysis further revealed that genes elevated pre-infection were enriched for pathways including cell cycle regulation, chromatin remodeling and protein ubiquitination (Fig. 4B). Conversely, genes upregulated post-infection were strongly associated with cytoplasmic translation, oxidative phosphorylation, ATP metabolic processes, and

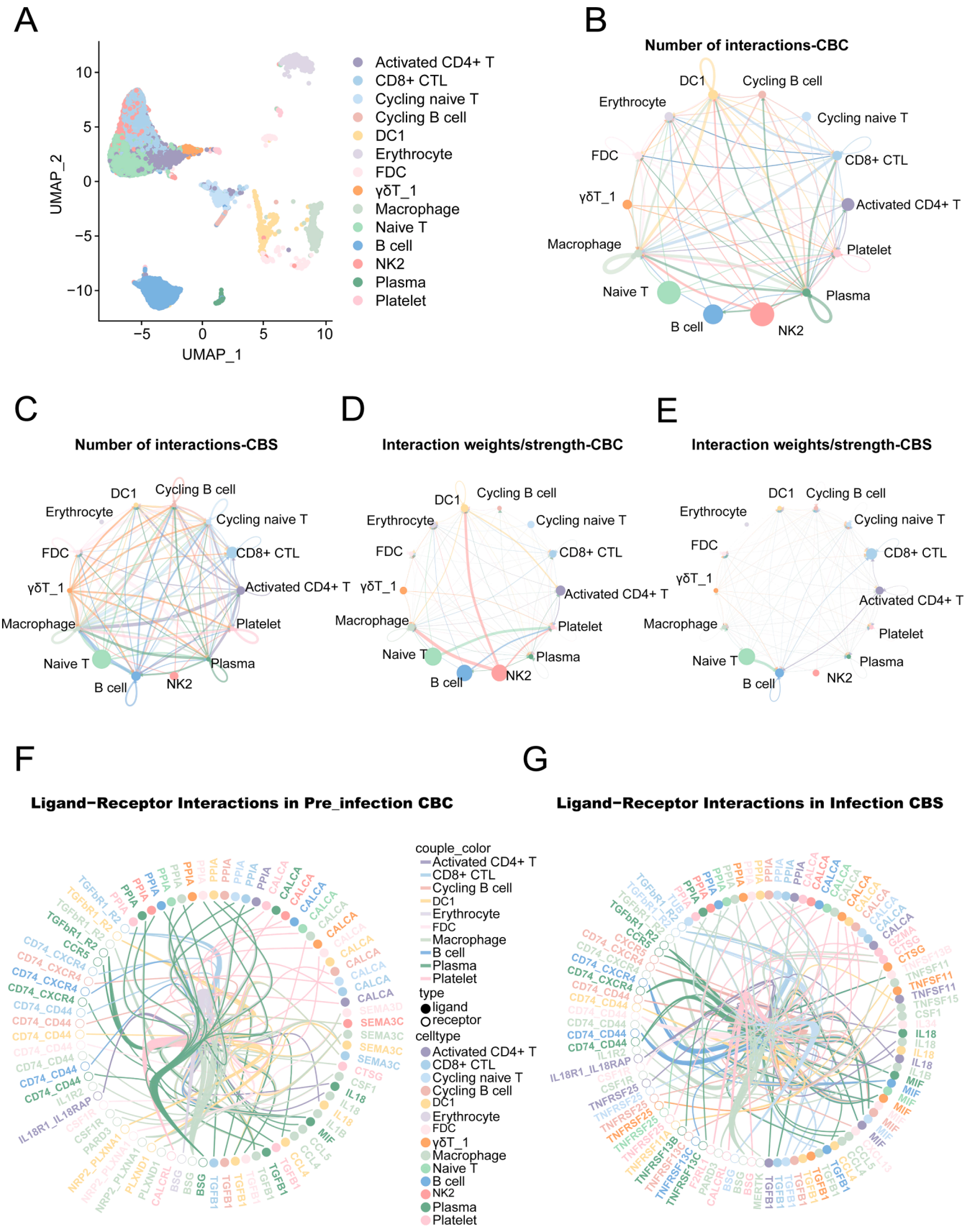

Fig. 2. Effects of *Salmonella* infection on spleen intercellular communication networks. (A) UMAP visualization of all cell clusters in Cobb broilers. (B-C) Circos plots showing the number of ligand-receptor (L-R) interactions in CBC(B) and CBS(C). (D-E) Network diagram of intercellular interaction strength in CBC(D) and CBS(E). (F-G) Chord diagram illustrating ligand-receptor interactions in CBC(F) and CBS(G), where colors represent distinct cell types and node shapes indicate interaction direction (filled circles, ligands; open circles, receptors).

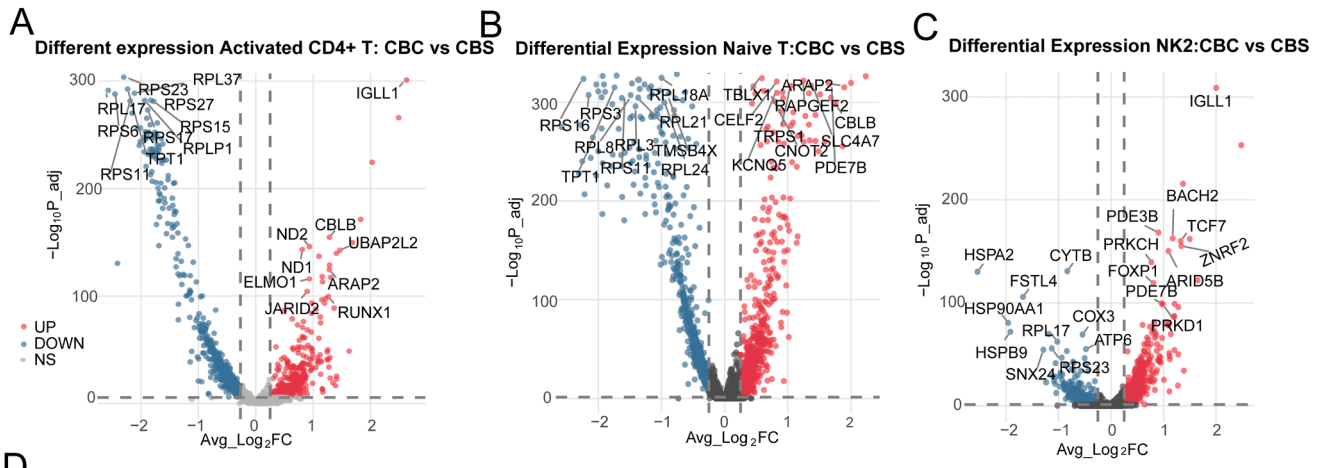

D

T cell	GO terms	
	CBC	LogP
Activated CD4+ T	cell population proliferation	-12.6
	regulation of small GTPase mediated signal transduction	-10.1
	T cell activation	-5.7
CD8+ CTL	cell surface receptor protein tyrosine kinase signaling pathway	-7.7
	cell activation	-4.8
	small GTPase-mediated signal transduction	-3.9
Cycling naïve T	neuron projection development	-6.6
	immune response-regulating cell surface receptor signaling pathway	-5.8
	heparan sulfate proteoglycan biosynthetic process	-5.7
Naïve T	ubiquitin-dependent protein catabolic process	-11.7
	regulation of autophagy	-11.1
	T cell receptor signaling pathway	-8.3
γδT_1	negative regulation of cell adhesion	-5.4
	N-glycan processing	-4.5
	regulation of muscle hypertrophy	-4.2
	CBS	LogP
Activated CD4+ T	cytoplasmic translation	-83.9
	proteolysis involved in protein catabolic process	-20.2
	apoptotic signaling pathway	-15.2
CD8+ CTL	cytoplasmic translation	-88.3
	regulation of apoptotic signaling pathway	-9.2
	alpha-beta T cell activation involved in immune response	-4.6
Cycling naïve T	protein-RNA complex assembly	-14.0
	protein folding	-13.3
	cellular response to cytokine stimulus	-10.2
Naïve T	cytoplasmic translation	-90.9
	oxidative phosphorylation	-34.3
	lymphocyte activation	-15.2
γδT_1	ribonucleoprotein complex biogenesis	-30.2
	regulation of intrinsic apoptotic signaling pathway	-10.7
	negative regulation of cellular component organization	-9.5

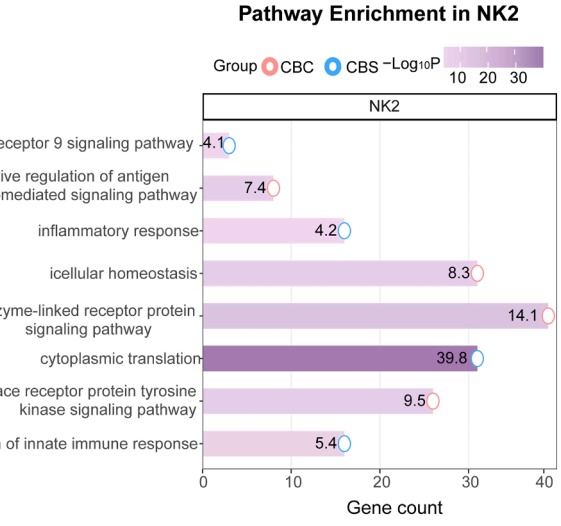

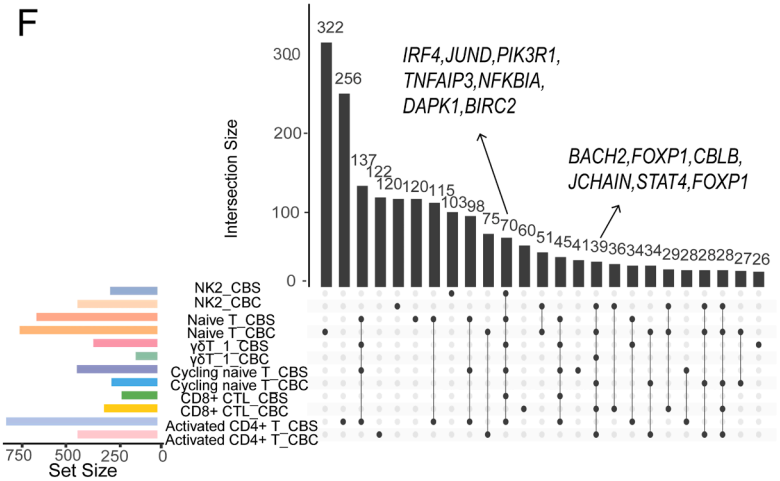

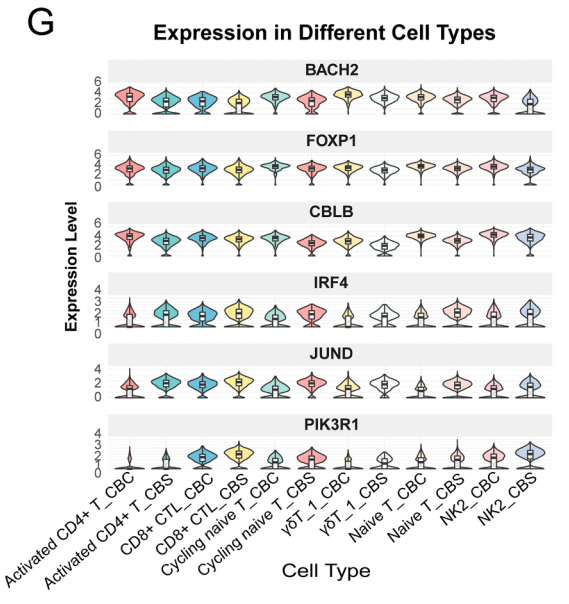

Fig. 3. Transcriptional alterations in T cell subsets and NK2 cells in Cobb broilers during *Salmonella* infection. (A-C) Volcano plots showing differentially expressed genes in Activated CD4+ T, Naïve T, and NK2 cells (CBC vs CBS). Genes with adjusted *p*-value <0.05 (Wilcoxon rank-sum test) and $\log_2$(fold change) > 0.25 were color coded. (D) Pathway enrichment analysis of DGEs of T cell subsets in CBC and CBS. (E) Pathway enrichment analysis of DEGs of NK2 cells in CBC and CBS. (F) Integrated comparative analysis of differentially expressed genes (DEGs) in T cell subsets and NK2 cells between CBC (Cobb broilers control) and CBS (Cobb broilers with *Salmonella* infection) states. (G) Violin plot of showing the expression across of a key genes cell types and conditions (CBC vs CBS).

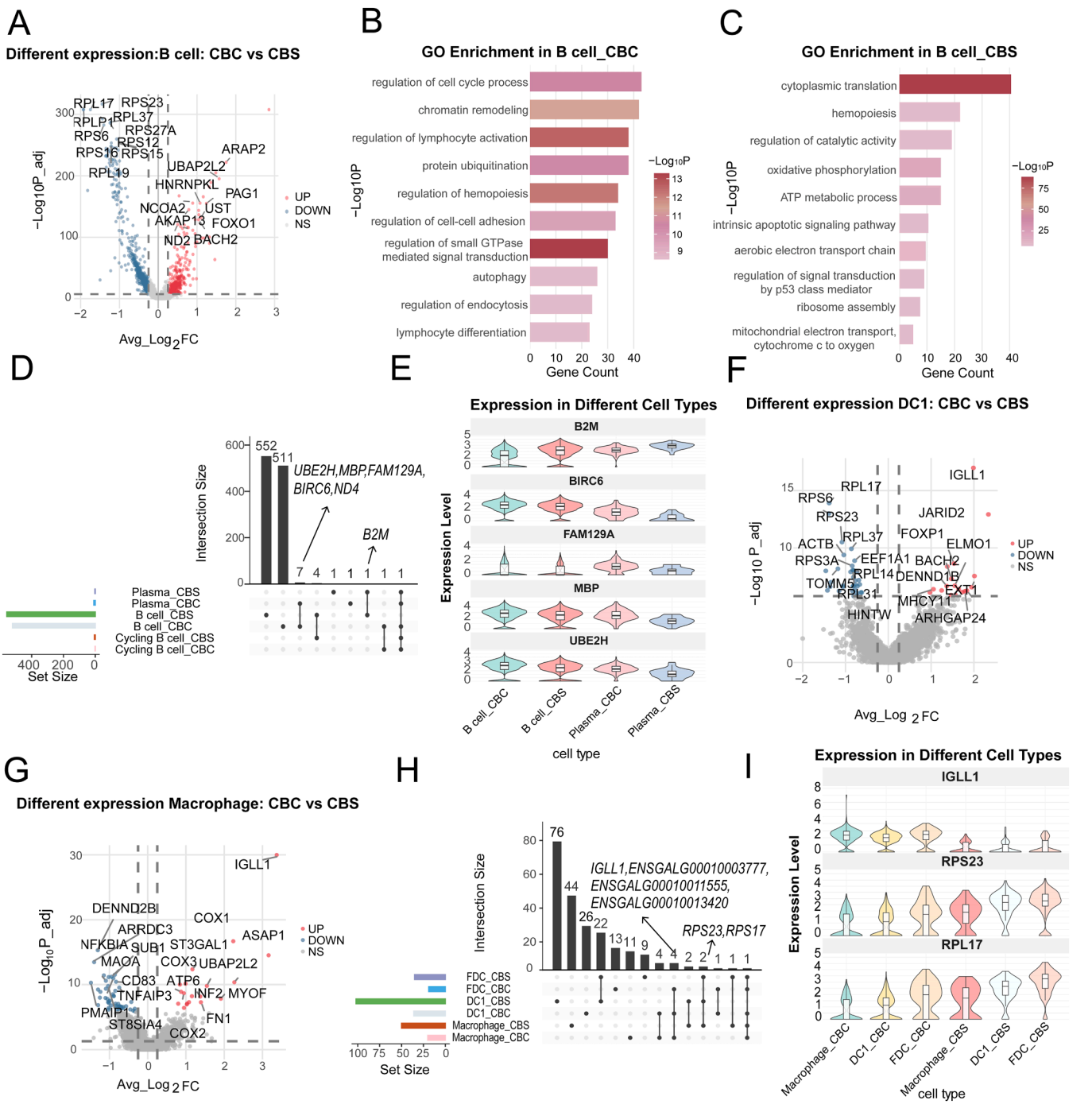

Fig. 4. Transcriptional alterations in B cell subsets and mononuclear phagocytes in Cobb broilers during*Salmonella* infection. (A) Volcano plots showing differentially expressed genes in B cells (CBC vs CBS). Genes with adjusted *p*-value <0.05 (Wilcoxon rank-sum test) and $\log_2$(fold change) > 0.25 were color coded. (B) Pathway enrichment analysis of up-regulated genes of B cells in CBC. (C) Pathway enrichment analysis of up-regulated genes of B cells in CBS. (D) Integrated comparative analysis of differentially expressed genes (DEGs) in B cell subsets between CBC (Cobb broilers control) and CBS (Cobb broilers with *Salmonella* infection) states. (E) Violin plot showing the expression of key genes in B cell subsets across the CBC and CBS. (F-G) Volcano plots showing differentially expressed genes in DC1 and Macrophage (CBC vs CBS) with the same statistical thresholds described in (A). (H) Integrated comparative analysis of differentially expressed genes (DEGs) in mononuclear phagocytes between CBC and CBS. (I) Violin plot showing the expression of key genes in mononuclear phagocytes subsets across the CBC and CBS.

ribosome assembly (Fig. 4C), reflecting heightened metabolic and translational activity upon infection. In plasma cells, only 10 differentially expressed genes were identified (Supplementary Fig. 3D). Comparative analysis of DEGs between B cells and plasma cells revealed 7 commonly upregulated genes before infection and only 1 shared upregulated gene after infection in both subsets (Fig. 4D). Among these shared genes, *UBE2H, MBP, BIRC6*, and *FAM129A* exhibited higher pre-infection expression relative to post-infection levels in both B cells and plasma cells (Fig. 4D and E). Among them, high *UBE2H* expression has been linked to global suppression of the immune microenvironment, including compromised antigen presentation by immune cells (Huang et al., 2025). By contrast, *B2M* was consistently upregulated after infection in both subsets (Fig. 4D and E), this gene encodes an essential component of major histocompatibility complex class I (MHC-I) (Gao et al., 2023), which specifically presents peptide antigens to the T cell receptors of CD8+ T cells (Wu et al., 2025).

In addition to lymphocytes, we profiled transcriptional alterations in myeloid cell subsets, including DC1, follicular dendritic cells (FDC) and macrophages, in response to *Salmonella* infection. During infection, macrophages, DC1 and FDC, respectively acquired 68, 52 and 137 DEGs (Fig. 4F-4G, Supplementary Fig. 3E, and Supplementary Table 2). Specifically, 19 and 49 DEGs were uniquely upregulated in macrophages pre- and post-infection, respectively, while DC1 exhibited 35 and 102, and FDC 18 and 34 lineage-specific upregulated DEGs (Fig. 4H). Notably, all myeloid subsets shared four commonly upregulated genes prior to infection, including *IGLL1*, whereas post-infection they coordinately upregulated a set of ribosome-related genes including *RPS23* and *RPL17*.

Breed-specific alterations in splenic intercellular communication and T cell gene expression patterns

Previous studies have reported that Cobb broilers and Beijing-You chicks exhibit distinct resistance to pathogenic bacterial infection (Elsharkawy et al., 2022). However, the differences in gene expression profiles of immune cells between these two breeds remain largely unclear. We analyzed single-cell transcriptomic data of immune cells from Beijing-You chicks control (BYC) and Cobb broilers control (CBC). To compares the inter-breed differences in immune characteristics under healthy conditions, we analyzed single-cell transcriptomic data of immune cells from BYC and CBC. The cell types detected in the two breeds were identical, including Activated CD4+ T, CD8+ CTL, Naïve T, B cell, Cycling B cell, Plasma, NK2, Macrophage, DC1, FDC, Erythrocyte, Platelet, and γδT_1 cell (Fig. 5A). However, Cobb broilers (CB) exhibited a higher proportion of CD8+ CTL (12.86% vs 1.99%) and Naïve T cells (32.26% vs 28.16%) but a lower proportion of B cells compared to Beijing-You chicks (BY) (17.64% vs 25.71%) (Supplementary Fig. 2C). To investigate whether there are differences in cell-cell interactions between different breeds, we systematically analyzed the intercellular communication networks in both breeds. The results showed that number of interactions between these two breeds was generally consistent. However, interaction weights varied across breeds (Fig. 5B and C). Specifically, interactions between DCs and NK cells, as well as those between DCs and activated T cells, were uniquely detected in Cobb broilers. At the ligand-receptor interaction level, Differences also exist between breeds. For example, TNFSF13B-TNFRSF13B/TNFRSF13C interaction from FDCs to B cells in BYC and IL18-IL18R1/ IL18RAP interaction from B/mononuclear phagocytes to T cell in CBC (Figs. 5D and 2F). T cell-intrinsic IL-18R signaling mounts a robust Th1 cognate response by driving proliferation and protecting against apoptosis (Oliveira et al., 2017).

Apart from the cell-cell communication, we further characterized transcriptional differences in immune cells between the two breeds. For T cells and NK cells, cycling naive T cells, activated CD4+ T, γδT_1 and CD8+ CTL exhibited fewer differentially expressed genes between the CB and BY, suggesting that the gene expression profiles of these cell types were relatively similar across breeds (Fig. 5E). In contrast, the gene expression patterns of naive T cells and NK2 cells differed the most between the two breeds (Fig. 5F). For naive T cells, there were 600 DEGs in CBC and BYC (Supplementary Table 3). Genes highly expressed in CBC were mainly enriched in cellular response to cytokine stimulus, regulation of leukocyte activation, whereas those highly expressed in BYC were mainly involved in regulation of cell activation and positive regulation of immune response (Fig. 5G and H). For NK2 cells, a total of 664 DEGs were identified, including several immune effector-related genes, *BACH2, PDCD1LG2, CTSH, TCF7*, and *FOXP1* (Fig. 5E and Supplementary Table 3). Genes upregulated in CBC were primarily associated with cell activation, leukocyte activation, and regulation of T cell receptor signaling (Fig. 5I), while those upregulated in Beijing-You chicks were mainly enriched in receptor-mediated signaling pathways and hemopoiesis (Fig. 5J). To further explore the consistency of breed-related differentially expressed genes across different cell types, we analyzed the corresponding gene sets. Our results showed that a total of 120 genes were specifically and highly expressed in NK2 cells of BYC. Sixty-five highly expressed genes were upregulated in both NK cells and naive T cells of BYC. Among T cell subsets, 121 genes were specifically highly expressed in naïve T cells of CBC (Fig. 5F). Furthermore, 72 highly expressed genes were shared between naïve T cells and γδT_1 cell in CBC (Fig. 5F). These results indicate that the expression differences of distinct cell types between breeds exhibit both commonalities and obvious cell-type specificity.

Breed-specific alterations in B cells and myeloid cells

We then compare the transcriptional characteristics of B cells and myeloid cells between BYC and CBC under healthy conditions, we first performed differential expression analysis on two B-cell subsets, B cells and Plasma cells. The results showed that transcriptional differences between the two chicken breeds were more pronounced in B cells (Fig. 6A). A total of 663 DEGs were identified, among which 292 were specifically upregulated in CBC and 344 were specifically upregulated in BYC (Fig. 6C and Supplementary Table 4). For example, ribosomal protein-related genes *RPS15, RPS12, RPS17, RPS24, RPS27A, RPL23,* and *RPL23A* exhibited significantly higher expression in CBC (Fig. 6A). Upregulated genes in CBC were mainly enriched in pathways related to regulation of T cell activation and cellular response to cytokine stimulus (Fig. 6E). In comparison, upregulated genes enriched in BYC were primarily associated with B cell activation and regulation of immune response (Fig. 6F). For Plasma cells, only 67 DEGs were detected, including 4 genes specifically upregulated in CBC and 36 in BYC (Fig. 6C and Supplementary Table 4). We further analyzed the overlap of differentially expressed genes in B cell subsets among different breeds. In BYC, a total of 17 genes were co-upregulated in both B cell and Plasma cells, including genes participated in B cell antigen receptor (BCR) signaling, such as *MEF2C* (Khiem et al., 2008), *PTPRJ* (Skrzypczynska et al., 2016), and *VAV3* (Inabe et al., 2002) (Fig. 6C and D). In CBC, a total of 3 genes were co-upregulated in both B cell and Plasma cells, including *CD63, IGLL1* and *GBP4L.1* (Fig. 6C and D).

We next examined transcriptional differences in myeloid cell populations between the two chicken breeds, including DC1 and Macrophage cells. In Macrophages, there were 66 DEGs between CBC and BYC (Fig. 6G and Supplementary Table 4). CBC showed significantly higher expression of *IGLL1, BF2, ATP11A, ADGRG2, RPL23*, and *PEL12* compared with BYC (Fig. 6G). Among these genes, *BF2* belongs to the MHC class I family and plays an essential role in antigen processing and presentation (Kim et al., 2018), whereas *RPL23* encodes a ribosomal protein involved in protein synthesis. In contrast, several genes were highly expressed in BYC Macrophages, including *PDE8A, MAP3K1, PPM1H, SLC9A9, CD200R1A, WNP1*, and *PLIN2* (Fig. 6G). For instance, *ABCA1* participates in lipid transport and cholesterol homeostasis and can influence macrophage foam cell formation and inflammatory phenotypes (Cao et al., 2025), suggesting that macrophages in CBC may exhibit enhanced activity in lipid metabolism regulation. In Macrophages, upregulated genes in BYC were mainly enriched in positive regulation of cell migration, enzyme-linked receptor protein signaling pathway and cellular homeostasis (Fig. 6K). In contrast, CBC upregulated genes were predominantly enriched in response to bacterium, fatty acid biosynthetic and metabolic process (Fig. 6L).

For DC1 cells, BYC exhibited higher expression of multiple genes, including *MEF2C, HSPB9, ERBB4*, and *BMPR2* (Fig. 6H and Supplementary Table 4). *ERBB4*, a member of the receptor tyrosine kinase family, regulates cell proliferation and differentiation (Frey et al., 2009). In DC1, upregulated genes in BYC were enriched in pathways associated with enzyme-linked receptor protein signaling pathway, regulation of hemopoiesis, immune response and T cell receptor signaling pathway (Fig. 6M and N). In contrast, upregulated genes in BYC were enriched in pathways of regulation of MAPK and NF-κB signaling and immune effector process (Fig. 6N). For example, DC1 in

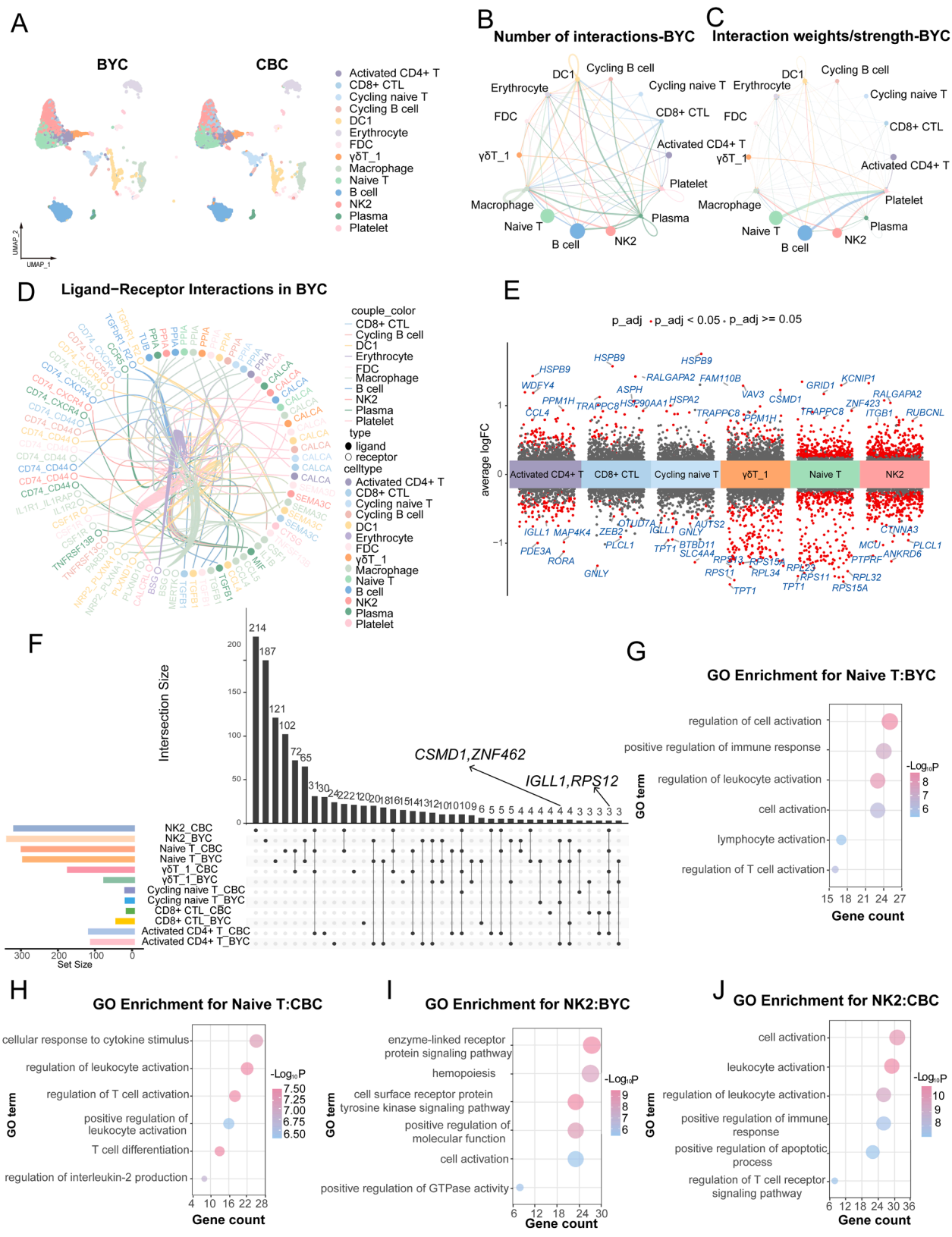

Fig. 5. Integrated analysis of splenic intercellular communication networks and transcriptional profiles of T/NK cell subsets between BYC and CBC. (A) UMAP plot of cell cluster distribution in BYC (Beijing-You chicks control) and CBC (Cobb broilers control) chicken spleen samples. (B) Network diagram of intercellular interaction number in BYC. (C) Network diagram of intercellular interaction strength in BYC. (D) Chord diagram illustrating ligand-receptor interactions in BYC where colors represent distinct cell types and node shapes indicate interaction direction (filled circles, ligands; open circles, receptors). (E) Volcano plots of differentially expressed genes in distinct T cell and NK cell subsets (Activated CD4+ T, CD8+ CTL, Cycling naive T, γδT_1, Naive T, NK2 cells) between BYC and CBC. Significant genes (adjusted p-value < 0.05, $\log_2$(fold change) > 0.25, Wilcoxon rank-sum test) are highlighted in color. (F) Integrated comparative analysis of differentially expressed genes (DEGs) in T cell subsets and NK2 cells between BYC and CBC. (G-J) Pathway enrichment analysis of DEGs of Naïve T and NK2 in BYC and CBC.

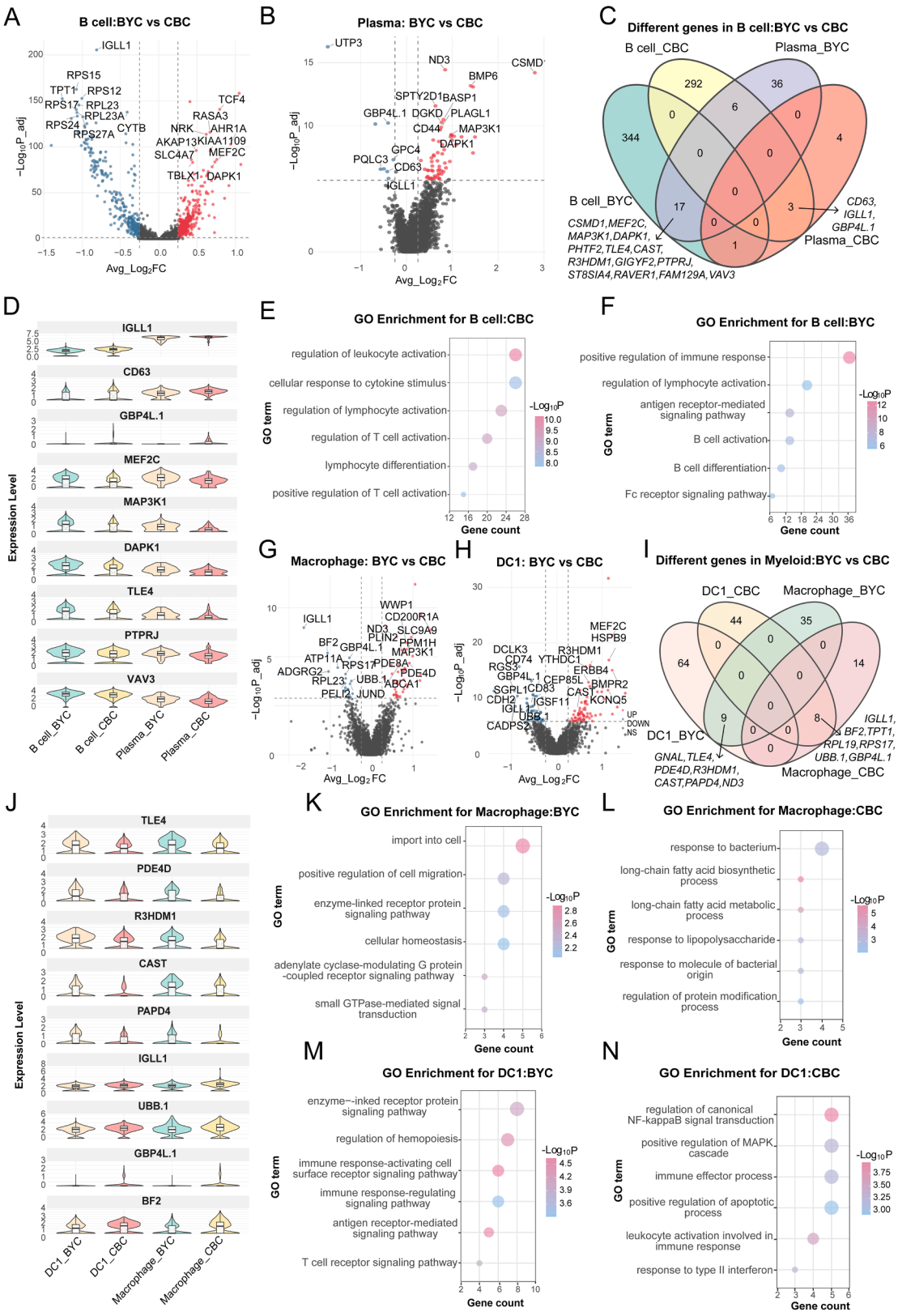

Fig. 6. Transcriptional alterations of B cell subsets and mononuclear phagocytes between Beijing-You chicks control (BYC) and Cobb broilers control (CBC). (A-B) Volcano plots showing differentially expressed genes in B cells and Plasma cells (BYC vs CBC). (C) Venn diagram showing the comparison of differentially expressed genes between BYC and CBC populations in B cell subsets. (D) Violin plot showing the expression of key genes in B cell subsets across the BYC and CBS conditions. (E-F) Pathway enrichment analysis of up-regulated genes of B cells from BYC and CBC. (G-H) Volcano plots showing differentially expressed genes in Macrophages and DC1 cells (BYC vs CBC). (I) Comparison of differentially expressed genes between BYC and CBC in mononuclear phagocytes. (J) Violin plot showing the expression of key genes in mononuclear phagocytes subsets across the BYC and CBC conditions. (K-N) Pathway enrichment analysis of DGEs of Macrophages and DC1 cells from BYC and CBC.

CBC displayed elevated expression of *CADPS2, GBP4L.1, CD74, RGS3, CDH2, UBB*, and *CD83* (Fig. 6H). *CD74* not only serves as the invariant chain of MHC class II molecules but also functions as a receptor for macrophage migration inhibitory factor (MIF), thereby participating in immune cell chemotaxis and activation (Bandola-Simon and Roche, 2026). *CD83*, a key marker of dendritic cell maturation, exerts immunostimulatory effects in its membrane-bound form by activating T cells and contributing to thymocyte development, whereas its soluble form has immunosuppressive properties (Prechtel and Steinkasserer, 2007).

To determine whether common transcriptional alterations existed between DC1 and Macrophages, we further examined overlapping DEGs between these two cell types (Fig. 6I). In BYC, nine genes were commonly upregulated in both DC1 and Macrophages, including *GNAL, TLE4, PDE4D, R3HDM1, CAST, PAPD4*, and *ND3* (Fig. 6I and J). Among them, *TLE4* participates in immune cell differentiation, *PDE4D* encodes a phosphodiesterase that regulates inflammatory responses through modulation of the cAMP signaling pathway, *R3HDM1* is involved in RNA processing, and *CAST* encodes a calpain inhibitor that contributes to cytoskeletal stability. By contrast, eight genes were commonly upregulated in CBC DC1 and Macrophages, including I*GLL1, BF2, TPT1, RPL19, RPS17, UBB.1*, and *GBP4L.1* (Fig. 6I and J). *BF2* participates in antigen processing and presentation (Miller and Taylor, 2016), *UBB.1* contributes to protein degradation and cellular homeostasis, and *GBP4L.1* is involved in interferon-induced innate immune responses (Park and Ryu, 2014; Tretina et al., 2019). Differential gene expression in innate immune cells across chicken breeds reflected divergent innate immune regulation. Based on these results, we performed a joint analysis of differentially expressed genes (DEGs) between CB and BY cell types, as well as DEGs in Cobb broilers before and after *Salmonella* infection. Across the 10 identified cell types, a total of 1,355 genes were common to both sets (Supplementary Table 5), which may represent key genes underlying the differential *Salmonella* resistance between breeds.

Discussion

In this study, we established a comprehensive single-cell transcriptomic atlas of the chicken spleen spanning embryonic to adult stages, comprising more than 92,691 single-cell profiles and identifying a total of 40 distinct cell types. Based on this atlas, we systematically compared the cellular composition of the chicken spleen across different developmental stages. In our dataset, the E16 time point exhibited a relatively low cell count, which is primarily attributed to limited cell capture efficiency at this stage. Following rigorous quality control, this dataset proved statistically sufficient to capture key cell types and dynamic changes, as evidenced by the high consistency of cell type annotation and the comparable proportions of major cell populations with E21(Fig. 1D). We then analyzed gene expression variations in splenic immune cells between diverse breeds, and further investigated transcriptomic changes in various immune cell populations before and after *Salmonella* infection. Our findings uncovered the shared regulatory patterns and cell type-specific characteristics underlying the immune responses against bacterial infection.

While T cell-mediated immunity is known to clear intracellular pathogens like *Salmonella* (Peres et al., 2021). Our single-cell analysis reveals a specific cellular mechanism underlying this process. We demonstrate that the host response is driven primarily by the transcriptional remodeling of naive T cells and activated CD4+ T cells, which exhibited the most abundant differentially expressed genes within the T cell compartment. Gene set enrichment analysis revealed that these subsets upregulate pathways related to T cell activation, oxidative phosphorylation, and protein translation, suggesting that metabolic reprogramming and biosynthetic capacity are prerequisites for their effector functions. This indicates that the functional competence of these specific subsets-rather than broad T cell activation-is the determining factor for effective bacterial clearance and immune homeostasis in the chicken spleen. As previously reported, CD4+ T cells can secrete a variety of cytokines and facilitate the activation of other immune cell populations, thereby critically contributing to host antibacterial immune defense (Lee, 2023). For example, Th1 cells and their secretion of TNF-α and IFN-γ are essential for macrophage activation, which represents a key process for efficient bacterial killing by the host (Hess et al., 1996; Ravindran et al., 2005; Tubo and Jenkins, 2014). Meanwhile, *IL-17A* produced by Th17 cells recruits neutrophils to the intestinal tract and modulates the expression of tight junction proteins in epithelial cells, thereby strengthening mucosal barrier protection (Raffatellu et al., 2008). In contrast, CD8+ T cells make only a limited contribution to *Salmonella* clearance (Takaya et al., 2019). Consistently, the gene expression profile of CD8+ T cells exhibited only minor alterations in our study. Besides, B cells exhibited prominent transcriptional changes before and after infection, suggesting that this population may represent a key regulatory group in the B-cell response to *Salmonella* infection. Following infection, B cells rapidly underwent transcriptional reprogramming and initiated differentiation programs. These processes contribute to antibody production and antigen presentation (Hua and Hou, 2020). Innate immune cells exert multiple effects during the early stage of *Salmonella* infection, as they not only directly suppress bacterial proliferation but also secrete cytokines and chemokines to activate and recruit inflammatory cells to infectious sites (Takaya et al., 2019). In our study, NK2 cells displayed markedly distinct gene expression profiles following *Salmonella* infection. Given the functional heterogeneity of these immune cell subsets, the differentially expressed genes following *Salmonella* infection were largely inconsistent across populations. However, we observed that several genes associated with protein translation were significantly upregulated across various immune cell subsets. Such widespread upregulation of ribosome assembly and translation-related genes following infection likely reflects the increased demand for protein synthesis accompanying the robust activation of immune cells. Activated immune cells require robust production of cytokines, chemokines, receptors, and effector molecules to mount an effective antibacterial response (Fitzgerald and Kagan, 2020). The upregulation of protein translation genes therefore represents a transcriptional adaptation to support elevated translation activity, which is essential for cell proliferation, activation, and the execution of antimicrobial immune functions (Tan et al., 2017). Furthermore, we observed that the expression of DEGs in response to *Salmonella* infection varied across multiple cell types and between breeds, exemplified by the *BF2* gene. *BF2* encodes a major histocompatibility complex (MHC) class I molecule, playing a dominant role in antigen presentation. This gene is characterized by high genetic diversity (Agulto et al., 2025), and the polymorphic nature of the chicken MHC is known to dictate resistance or susceptibility to various infectious pathogens (Wallny et al., 2006). Consequently, these variations likely represent a key genetic mechanism underlying the observed differences in disease resistance between breeds.

In addition to the observed differences in gene expression profiles, our analysis further revealed significantly enhanced cellular crosstalk among lymphoid cells, as well as between lymphoid and myeloid lineages following *Salmonella* infection. These interactions included crosstalk between follicular dendritic cells (FDCs) and B cells, as well as between T cells and B cells. FDCs have been reported to attract B cells and specific T cell subsets into lymphoid follicles and support B cell survival within germinal centers (Heesters et al., 2014). Moreover, the crosstalk between helper T cells and B cells is critical for initiating T cell-dependent antibody responses, which constitutes a core mechanism of protective immunity (Petersone et al., 2018). The strengthened intercellular communication between these immune compartments likely facilitates coordinated signal transduction, efficient antigen presentation, and synergistic activation of both innate and adaptive immune programs, thereby enhancing host resistance to *Salmonella* invasion and reinforcing systemic immune defense.

In summary, our study delineated the dynamic cellular composition of the chicken spleen across embryonic to adult developmental stages at

single-cell resolution, revealing stage-specific characteristics of immune cell. Upon *Salmonella* infection, we further identified dramatic transcriptional remodeling in diverse immune subsets, accompanied by markedly enhanced intercellular crosstalk within immune cell compartments. These integrated results highlight the coordinated shifts in gene expression programs, and cell-cell communication networks that underpin antibacterial defense of the splenic immune system.

Conclusion

In summary, this study presents a high-resolution, spatiotemporal single-cell atlas of the chicken spleen, elucidating the developmental trajectories of immune cells from embryogenesis to adulthood. Beyond characterizing cellular dynamics, our integrated analysis of *Salmonella* infection and breed-specific differences reveals that variations in gene expression patterns and cellular interaction networks contribute to the divergent disease resistance phenotypes. These findings not only elucidate the splenic immune landscape in birds but also nominate actionable molecular targets within specific cell types that could be leveraged for genetic selection and precision breeding programs aimed at enhancing poultry resilience to bacterial pathogens.

Funding sources

This work was supported by the National Natural Science Foundation of China (Grant No. 32302733) and China Postdoctoral Science Foundation (Grant No. 2023M742864) and Shaanxi Provincial Postdoctoral Science Foundation (Grant No. 2023BSHYDZZ86).

CRediT authorship contribution statement

Ping Wang: Writing – original draft, Visualization, Methodology, Formal analysis. **Ruizhi Chen:** Visualization, Methodology, Formal analysis, Data curation. **Kai Ren:** Methodology. **Xinyu Pu:** Data curation. **Jilong Ren:** Methodology. **Wuqiang Huo:** Methodology. **Fei Wang:** Writing – review & editing, Supervision, Resources, Funding acquisition, Conceptualization.

Disclosures

The authors declare that they have no known competing financial interests or personal relationships that could have appeared to influence the work reported in this paper.

Acknowledgments

We thank the High-Performance Computing platform of Northwest A&F University for providing computing resources.

Supplementary materials

Supplementary material associated with this article can be found, in the online version, at doi:10.1016/j.psj.2026.107173.

Supplementary Fig. 1. Quality control and cell type annotation of single-cell RNA sequencing (scRNA-seq) data from chicken spleen. (A) Violin plots showing the distribution of the number of nFeature_RNA (left) and nCount_RNA (right) across all cells. (B) Dot plot showing the expression pattern (average expression and percentage of expression) of representative marker genes in major cell types annotated in the spleen. (C) Stacked bar plot illustrating the proportion of each cell type in the spleen across the three chicken breeds: from left to right, Cobb broilers (CB), Hy-Line Brown (HLB), and Beijing-You chicks (BY).

Supplementary Fig. 2. Transcriptomic landscape and cell type proportions of spleen immune cells in Cobb broilers (control vs *Salmonella*-infected) and two chicken breeds (Beijing-You chicks vs Cobb broilers). (A) Heatmap of the top 50 marker genes for each cell type, with each column representing a cell type and each row representing a gene. (B) Relative proportions of each immune cell population in CBC (Cobb broilers control) and CBS (Cobb broilers with *Salmonella* infection). (C) Stacked bar chart illustrating the relative proportions of each cell population in BY (Beijing-You chicks) and CB (Cobb broilers).

Supplementary Fig. 3. Differential gene expression profiles in distinct immune cell subsets of chicken spleen between CBC (Cobb broilers control) and CBS (Cobb broilers with *Salmonella* infection) groups. (A-E) Volcano plots showing differentially expressed genes in γδT_1, Cycling naïve T, CD8+ CTL, Plasma and FDC cells (CBC vs CBS). Genes with adjusted p-value <0.05 (Wilcoxon rank-sum test) and $\log_2$(fold change) > 0.25 were color coded.

Supplementary Fig. 4. GO functional enrichment analysis of differentially expressed genes in key T cell subsets between Beijing-You chicks (BYC) and Cobb broilers (CBC). (A-F) Bubble plots illustrating the top GO terms enriched in CD8+ CTL, γδT_1, and Activated CD4+ T cell subsets from BYC and CBC chickens, respectively. Bubble size indicates the number of enriched genes, and color gradient represents the enrichment significance (-$\log_{10}p$-value).

References

Agulto, T.N., Kim, M., Manjula, P., Fernando, R., Kaufman, J., Lee, J.H., 2025. Genetic insights into the major histocompatibility complex class I BF2 gene of Korean native chickens in relation to the LEI0258 microsatellite marker and the 90-SNP panel. Immunogenetics 77, 31.

Bandola-Simon, J., Roche, P.A., 2026. MHC Class II and beyond: complex role of CD74 in cancer. Cells 15, 128.

Barrow, P.A., Neto, O.F., 2011. Pullorum disease and fowl typhoid—New thoughts on old diseases: a review. Avian Pathol. 40, 1–13.

Butler, A., Hoffman, P., Smibert, P., Papalexi, E., Satija, R., 2018. Integrating single-cell transcriptomic data across different conditions, technologies, and species. Nat. Biotechnol. 36, 411–420.

Cao, L., Zhang, J., Yu, L., Yang, W., Qi, W., Ren, R., Liu, Y., Hou, Y., Cao, Y., Li, Q., 2025. E3 ubiquitin ligase Listerin regulates macrophage cholesterol efflux and atherosclerosis by targeting ABCA1. J. Clin. Invest. 135 (16), e186509.

Doan, T.A., Forward, T.., Tamburini, B.A.J., 2022. Trafficking and retention of protein antigens across systems and immune cell types. Cell Mol. Life Sci. 79, 275.

Elsharkawy, M.S., Wang, H., Ding, J., Madkour, M., Wang, Q., Zhang, Q., Zhang, N., Li, Q., Zhao, G., Wen, J., 2022. Transcriptomic analysis of the spleen of different chicken breeds revealed the differential resistance of *Salmonella* typhimurium. Genes Basel 13 (5), 811.

Fitzgerald, K.A., Kagan, J.C., 2020. Toll-like receptors and the control of immunity. Cell 180, 1044–1066.

Frey, M.R., Edelblum, K.L., Mullane, M.T., Liang, D., Polk, D.B., 2009. The ErbB4 growth factor receptor is required for colon epithelial cell survival in the presence of TNF. Gastroenterology 136, 217–226.

Gao, Y., Hong, Y., Huang, L., Zheng, S., Zhang, H., Wang, S., Yao, Y., Zhao, Y., Zhu, L., Xu, Q., 2023. β2-microglobulin functions as an endogenous NMDAR antagonist to impair synaptic function. Cell 186, 1026–1038.e20 e20.

Golub, R., Tan, J., Watanabe, T., Brendolan, A., 2018. Origin and immunological functions of spleen stromal cells. Trends Immunol. 39, 503–514.

Guo, R., Xie, X., Ren, Q., Liew, P.X., 2025. New insights on extramedullary granulopoiesis and neutrophil heterogeneity in the spleen and its importance in disease. J. Leukoc. Biol. 117, qiae220.

Gutiérrez-Vázquez, C., Rodríguez-Galán, A., Fernández-Alfara, M., Mittelbrunn, M., Sánchez-Cabo, F., Martínez-Herrera, D.J., Ramírez-Huesca, M., Pascual-Montano, A., Sánchez-Madrid, F., 2017. miRNA profiling during antigen-dependent T cell activation: a role for miR-132-3p. Sci. Rep. 7, 3508.

Heesters, B.A., Myers, R.C., Carroll, M.C., 2014. Follicular dendritic cells: dynamic antigen libraries. Nat. Rev. Immunol. 14, 495–504.

Hess, J., Ladel, C., Miko, D., Kaufmann, S.H., 1996. *Salmonella* typhimurium aroA- infection in gene-targeted immunodeficient mice: major role of CD4+ TCR-αβ cells and IFN-γ in bacterial clearance independent of intracellular location. J. Immunol. 156, 3321–3326.

Hua, Z., Hou, B., 2020. The role of B cell antigen presentation in the initiation of CD4+ T cell response. Immunol. Rev. 296, 24–35.

Huang, F., Zhang, Z., Fang, J., Chen, Y., Wei, J., Li, Q., Zhang, C., Huang, S., Hou, B., 2025. Integrated scRNA-seq and transcriptome analyses uncover the effects of UBE2H on the immune microenvironment regulation in pancreatic cancer. Cancer Cell Int. 25, 422.

Igarashi, K., Ochiai, K., Itoh-Nakadai, A., Muto, A., 2014. Orchestration of plasma cell differentiation by Bach2 and its gene regulatory network. Immunol. Rev. 261, 116–125.

Inabe, K., Ishiai, M., Scharenberg, A.M., Freshney, N., Downward, J., Kurosaki, T., 2002. Vav3 modulates B cell receptor responses by regulating phosphoinositide 3-kinase activation. J. Exp. Med. 195, 189–200.

Jin, S., Guerrero-Juarez, C.F., Zhang, L., Chang, I., Ramos, R., Kuan, C.-H., Myung, P., Plikus, M.V., Nie, Q., 2021. Inference and analysis of cell-cell communication using CellChat. Nat. Commun. 12, 1088.
Jo, S., Ohara, R.A., Theisen, D.J., Kim, S., Liu, T., Bullock, C.B., He, M., Ou, F., Chen, J., Piersma, S.J., 2025. Shared pathway of WDFY4-dependent cross-presentation of immune complexes by cDC1 and cDC2. J. Exp. Med. 222 (4), e20240955.
Khiem, D., Cyster, J.G., Schwarz, J.J., Black, B.L., 2008. A p38 MAPK-MEF2C pathway regulates B-cell proliferation. Proc. Natl. Acad. Sci. 105, 17067–17072.
Kim, T., Hunt, H.D., Parcells, M.S., van Santen, V., Ewald, S.J., 2018. Two class I genes of the chicken MHC have different functions: BF1 is recognized by NK cells while BF2 is recognized by CTLs. Immunogenetics 70, 599–611.
Korsunsky, I., Millard, N., Fan, J., Slowikowski, K., Zhang, F., Wei, K., Baglaenko, Y., Brenner, M., Loh, P.R., Raychaudhuri, S., 2019. Fast, sensitive and accurate integration of single-cell data with Harmony. Nat. Methods 16, 1289–1296.
Lee, G.R., 2023. Molecular mechanisms of T helper cell differentiation and functional specialization. Immune Netw. 23, e4.
Li, Y., Li, Y., Xu, S., Chen, Y., Zhou, P., Hu, T., Li, H., Liu, Y., Xu, Y., Ren, J., 2022. N-acylethanolamine acid amidase (NAAA) exacerbates psoriasis inflammation by enhancing dendritic cell (DCs) maturation. Pharmacol. Res. 185, 106491.
Matulova, M., J. Rajova, L. Vlasatikova, J. Volf, H. Stepanova, H. Havlickova, F. Sisak, and I. Rychlik. 2012. Characterization of chicken spleen transcriptome after infection with *Salmonella* enterica serovar Enteritidis.
Miller, M.M., Taylor, R.L., 2016. Brief review of the chicken major histocompatibility complex: the genes, their distribution on chromosome 16, and their contributions to disease resistance. Poult. Sci. 95, 375–392.
Nadukkandy, A.S., Kalaiselvan, S.., Lin, L., Luo, Y., 2025. Clinical application of single-cell RNA sequencing in disease and therapy. Clin. Transl. Med. 15, e70512.
Nayar, R., Enos, M., Prince, A., Shin, H., Hemmers, S., Jiang, J., Klein, U., Thomas, C.J., Berg, L.J., 2012. TCR signaling via Tec kinase ITK and interferon regulatory factor 4 (IRF4) regulates CD8+ T-cell differentiation. Proc. Natl. Acad. Sci. 109, E2794–E2802.
Oliveira, A.-C., Gomes-Neto, J.F., Barbosa, C.-H.D., Granato, A., Reis, B.S., Santos, B.M., Fucs, R., Canto, F.B., Nakaya, H.I., Nobrega, A., 2017. Crucial role for T cell-intrinsic IL-18R-MyD88 signaling in cognate immune response to intracellular parasite infection. Elife 6, e30883.
Oshota, O., Conway, M., Fookes, M., Schreiber, F., Chaudhuri, R.R., Yu, L., Morgan, F.J. E., Clare, S., Choudhary, J., Thomson, N.R., Lio, P., Maskell, D.J., Mastroeni, P., Grant, A.J., 2017. Transcriptome and proteome analysis of *Salmonella* enterica serovar typhimurium systemic infection of wild type and immune-deficient mice. PLoS One 12, e0181365 e0181365.
Pan, T., Dong, Z., Zhang, H., Yang, F., Chen, Y., 2025. Single-cell sequencing reveals cellular heterogeneity and molecular mechanisms in tendon and enthesis injury repair. Front. Physiol. 16, 1685955.
Papalexi, E., Satija, R., 2018. Single-cell RNA sequencing to explore immune cell heterogeneity. Nat. Rev. Immunol. 18, 35–45.
Park, C.W., Ryu, K.Y., 2014. Cellular ubiquitin pool dynamics and homeostasis. BMB Rep. 47, 475–482.
Peres, N.G., Wang, N., Whitney, P., Engel, S., Shreenivas, M.M., Comerford, I., Hocking, D.M., Erazo, A.B., Förster, I., Kupz, A., 2021. CD4+ T cell immunity to *Salmonella* is transient in the circulation. PLoS Pathog. 17, e1010004 e1010004.
Petersone, L., Edner, N.M., Ovcinnikovs, V., Heuts, F., Ross, E.M., Ntavli, E., Wang, C.J., Walker, L.S.K., 2018. T cell/B cell collaboration and autoimmunity: an intimate relationship. Front. Immunol. 9, 1941.
Prechtel, A.T., Steinkasserer, A., 2007. CD83: an update on functions and prospects of the maturation marker of dendritic cells. Arch. Dermatol. Res. 299, 59–69.
Qiu, X., Mao, Q., Tang, Y., Wang, L., Chawla, R., Pliner, H.A., Trapnell, C., 2017. Reversed graph embedding resolves complex single-cell trajectories. Nat. Methods 14, 979–982.
Raffatellu, M., Santos, R.L., Verhoeven, D.E., George, M.D., Wilson, R.P., Winter, S.E., Godinez, I., Sankaran, S., Paixao, T.A., Gordon, M.A., 2008. Simian immunodeficiency virus–induced mucosal interleukin-17 deficiency promotes *Salmonella* dissemination from the gut. Nat. Med. 14, 421–428.
Ravindran, R., Foley, J., Stoklasek, T., Glimcher, L.H., McSorley, S.J., 2005. Expression of T-bet by CD4 T cells is essential for resistance to *Salmonella* infection. J. Immunol. 175, 4603–4610.
Rolland, D.C., Basrur, V., Conlon, K., Wolfe, T., Fermin, D., Lim, M.S., Elenitoba-Johnson, K.S., 2011. Global phosphoproteomic analysis of B-cell lymphoma signatures reveals the role of active B-cell receptor signaling in germinal center derived NHLs. Blood 118, 583.
Sharma, S., Kaur, S., Naguib, M., Bragg, A., Schneider, A., Kulkarni, R.R., Nazmi, A., Abdelaziz, K., 2025. Major foodborne bacterial pathogens in poultry: implications for human health and the poultry industry and probiotic mitigation strategies. Microorganisms 13, 2363.
Skrzypczynska, K.M., Zhu, J.W., Weiss, A., 2016. Positive regulation of Lyn kinase by CD148 is required for B cell receptor signaling in B1 but not B2 B cells. Immunity 45, 1232–1244.
Szydłowski, M., Jabłońska, E., Juszczyński, P., 2014. FOXO1 transcription factor: a critical effector of the PI3K-AKT axis in B-cell development. Int. Rev. Immunol. 33, 146–157.
Takaya, A., Yamamoto, T., Tokoyoda, K., 2019. Humoral immunity vs. *Salmonella*. Front. Immunol. 10, 3155.
Tan, H., Yang, K., Li, Y., Shaw, T.I., Wang, Y., Blanco, D.B., Wang, X., Cho, J.H., Wang, H., Rankin, S., Guy, C., Peng, J., Chi, H., 2017. Integrative proteomics and phosphoproteomics profiling reveals dynamic signaling networks and bioenergetics pathways underlying T cell activation. Immunity 46, 488–503.
Tretina, K., Park, E.S., Maminska, A., MacMicking, J.D., 2019. Interferon-induced guanylate-binding proteins: guardians of host defense in health and disease. J. Exp. Med. 216, 482–500.
Tubo, N.J., Jenkins, M.K., 2014. CD4+ T cells: guardians of the phagosome. Clin. Microbiol. Rev. 27, 200–213.
Tzec-Interián, J.A., González-Padilla, D., Góngora-Castillo, E.B., 2025. Bioinformatics perspectives on transcriptomics: a comprehensive review of bulk and single-cell RNA sequencing analyses. Quant. Biol. 13, e78.
Valatas, V., Kolios, G., Bamias, G., 2019. TL1A (TNFSF15) and DR3 (TNFRSF25): a co-stimulatory system of cytokines with diverse functions in gut mucosal immunity. Front. Immunol. 10, 421466.
Wallny, H.J., Avila, D., Hunt, L.G., Powell, T.J., Riegert, P., Salomonsen, J., Skjødt, K., Vainio, O., Vilbois, F., Wiles, M.V., Kaufman, J., 2006. Peptide motifs of the single dominantly expressed class I molecule explain the striking MHC-determined response to Rous sarcoma virus in chickens. Proc. Natl. Acad. Sci. U. A. 103, 1434–1439.
Wang, Z., Ji, X., Zhang, Y., Yang, F., Su, H., Zhang, H., Li, Z., Zhang, W., Sun, W., 2024. Interactions between LAMP3+ dendritic cells and T-cell subpopulations promote immune evasion in papillary thyroid carcinoma. J. Immunother. Cancer 12, e008983 e008983.
Wang, F., Ren, J., Zhou, Y., Huo, W., Liu, H., Qin, M., Jing, Y., Yin, Z., Shi, T., Shan, H., Tan, G., Wang, H., Guo, X., Mei, J., Yue, Z., Hou, Z., Zhou, H., Song, J., Degn, S.E., Lin, L., Luo, Y., Meng, F., Fang, X., Zhang, H., He, X., Fang, L., Jiang, Y., 2026. Cross-species comparison of amniote single-cell transcriptomes reveals evolutionary conservation and divergence in the chicken immune system. Nat Commun.
Wigley, P., 2014. *Salmonella* enterica in the chicken: how it has helped our understanding of immunology in a non-biomedical model species. Front. Immunol. 5, 482.
Wu, Y., Sun, Z., Xia, L., Tian, P., Jiao, L., Li, Y., Wei, Z., Wang, X., Li, X., Zhang, G., 2025. MHC-I pathway disruption by viruses: insights into immune evasion and vaccine design for animals. Front. Immunol. 16, 1540159.
Xie, L., Tao, Y., Shen, Z., Deng, H., Duan, X., Xue, Y., Chen, D., Li, Y., 2024. Congenital asplenia impairs heme-iron recycling during erythropoiesis in zebrafish. Dev. Comp. Immunol. 151, 105108.
Zeng, J., Yi, D., Sun, W., Liu, Y., Chang, J., Zhu, L., Zhang, Y., Pan, X., Dong, Y., Zhou, Y., 2021. Overexpression of HOXA9 upregulates NF-κb signaling to promote human hematopoiesis and alter the hematopoietic differentiation potentials. Cell Regen. 10, 9.
Zhang, Q., Wang, Q., Zheng, J., Zhang, J., Zhang, G., Ying, F., Liu, D., Wen, J., Li, Q., Zhao, G., 2025. Single-cell RNA sequencing of the spleen reveals differences in *Salmonella* typhimurium infection mechanisms between different chicken breeds. Poult. Sci. 104, 104669.
Zhou, Y., Zhou, B., Pache, L., Chang, M., Khodabakhshi, A.H., Tanaseichuk, O., Benner, C., Chanda, S.K., 2019. Metascape provides a biologist-oriented resource for the analysis of systems-level datasets. Nat. Commun. 10, 1523.